Computational Materials Science 50 (2011) 3101–3104

Contents lists available at ScienceDirect

Computational Materials Science

journal homepage: www.elsevier.com/locate/commatsci

Ab initio calculations of the hydroxyl impurities in BaF_2

Hongting Shi [a], Yan Wang [b,*], Ran Jia [c], Roberts I. Eglitis [d]

[a] School of Science, Beijing Institute of Technology, 100081 Beijing, PR China
[b] Gansu Civil Engineering Research Institute, 730020 Gansu Lanzhou, PR China
[c] Department of Mathematics and Natural Sciences, Bergische Universität Wuppertal, D-42097 Wuppertal, Germany
[d] Institute of Solid State Physics, University of Latvia, 8 Kengaraga Str., Riga LV1067, Latvia

ARTICLE INFO

Article history:
Received 10 February 2011
Received in revised form 17 May 2011
Accepted 19 May 2011
Available online 14 June 2011

Keywords:
DFT-B3PW
Hydroxyl impurity
Barium fluoride
Electronic structure
Band structure
DOS

ABSTRACT

OH^- impurities in BaF_2 crystal have been studied by using density functional theory (DFT) with hybrid exchange potentials, namely DFT-B3PW. Three different configurations of OH^- impurities were investigated and the (1 1 1)-oriented OH^- configuration is the most stable one. Our calculations show that OH^- as an atomic group has a steady geometrical structure instead of electronic properties in different materials. The studies on band structures and density of states (DOS) of the OH^--impurity systems indicate that there are two defect levels induced by OH^- impurities. The two superposed occupied OH^--bands located 1.95 eV above the valance bands (VB) at Γ point mainly consist of the O *p* orbitals, and the H *s* orbitals do the major contribution to the empty defect level located 0.78 eV below the conduction bands (CB). The optical absorption due to the doped OH^- is centered around 8.61 eV.

1. Introduction

Alkaline-earth fluorides such as CaF_2 and BaF_2, whose band gaps are larger than 10 eV, are very important for many optical applications. As an example, a recent demand for lens materials available in short wavelength lithography is a typical application. The currently targeted wavelength is 157 nm (about 8 eV) from an F_2-excimer laser. This wavelength is far shorter than the transparent region of quartz that is the most popular optical material in the ultraviolet (UV) region. Additionally, for BaF_2, it is the fastest luminescent material that has been found to date [1]. Recently, BaF_2 has also been found to exhibit superionic conductivity by dissolving appropriate impurities into the lattice or by introducing an interface that causes the redistribution of ions in the space charge region, and is therefore considered as a candidate material for high-temperature batteries, fuel cells, chemical filters and sensors [2]. Considering the high technological importance of alkaline-fluorides, it is not surprising that during the last years, they have been the subject of many experimental and theoretical studies [3–27].

It is well known that optical and mechanical properties of crystals are strongly affected by defects and impurities unavoidably present in any real material. Contemporary knowledge of defects in solids has helped to create a field of technology, namely *defect engineering*, which is aimed at manipulating the nature and concentration of defects in a material so as to tune its properties in a desired manner or to generate different behaviors. BaF_2 could become important optical materials if one could avoid or, at least, control the photoinduced defect formation, which so far in applications degrades its optical quality. Therefore, it is significative to understand the nature of defects in BaF_2.

Coloration effects in alkaline-earth fluorides are strongly influenced by some impurities. Investigations by Adler and Kveta [28] and Bontinck [29] show that alkaline-earth fluorides reacts readily with water vapor at high temperatures and suggest that the resulting hydrolysis gives rise to a variety of defects which includes O^{2-} ions in fluorine sites and charge-compensating fluorine vacancies, hydrogen impurities dissolved as H_s^- ions in fluorine sites and as H_i^0 in interstitial sites, as well as OH^- impurities. One of the big unsolved problems in the context of the application of alkaline-earth fluorides as optical materials is these contaminations in the crystals. As an extension of our previous studies dealing with oxygen and hydrogen impurities in BaF_2, we performed calculations for OH^- impurities in BaF_2 crystal.

2. Calculation method

It is well known that the HF method considerably overestimates the optical band gap and density functional theory (DFT)

* Corresponding author.
E-mail address: yanwang.gansu@gmail.com (Y. Wang).

0927-0256/$ - see front matter © 2011 Elsevier B.V. All rights reserved.
doi:10.1016/j.commatsci.2011.05.033

underestimates it. To study the hydroxyl (OH^-) impurities in BaF_2 crystal, we applied the first-principles hybrid DFT-B3PW method, according to our previous studies dealing with CaF_2, BaF_2 and SrF_2 perfect crystals, which gave the best agreement with experiments for the lattice constants, bulk modulus and optical band gaps. The hybrid exchange–correlation B3PW functional involves a hybrid of nonlocal Fock exact exchange, local density approximation (LDA) exchange, and Becke's gradient-corrected exchange functional [30] combined with the nonlocal gradient-corrected correlation potential by Perdew and Wang [31–33]. All numerical calculations on OH^- impurities in BaF_2 crystal were performed by the CRYSTAL-2006 computer code [34]. The CRYSTAL-2006 code employs Gaussian-type functions (GTF) localized at atoms as the basis for an expansion of the crystalline orbitals. In order to employ the LCAO-GTF (linear combination of atomic orbitals) method, it is desirable to have optimized basis sets (BS). In our calculations for fluorine atoms, we applied the basis set developed by Catti et al. [5]. For Ba, the BS optimization for $BaTiO_3$ perovskite was developed and discussed in [35,36]. The Hay–Wadt small-core effective core pseudopotential (ECP) was adopted for the Ba atom [37]. The small-core ECP replaces only inner core or bitals, but orbitals for subvalence electrons as well as for valence electrons are calculated self-consistently. In this paper, we used this BS for Ba. The hydroxyl consists of an oxygen atom and a hydrogen atom. In our calculations, the BS for O given in the Basis Sets Library [34] and for H developed by Dovesi et al. [38] were adopted. The basis sets are believed to be transferable, so that, once determined for some chemical constituents, they may be applied successfully in calculations for a variety of chemical substances where the latter participates.

The reciprocal space integration was performed by sampling the Brillouin zone of the 96-atom supercell with $4 \times 4 \times 4$ Pack–Monkhorst net [39]. The thresholds N (i.e., the calculation of integrals with an accuracy of 10^{-N}) in our calculations were chosen as a compromise between the accuracy of calculations and the large computational time for large supercells. They are 7, 7, 7, 7 and 14 for the Coulomb overlap, Coulomb penetration, exchange overlap, the first-exchange pseudo-overlap and the second-exchange pseudo-overlap, respectively [40]. For the lattice constant (a_0) of BaF_2, we used our theoretical optimized value of 6.26 Å.

To simulate OH^- impurities in BaF_2, we replaced one fluorine atom with an oxygen atom and inserted a hydrogen atom into an atomic interstitial site near the oxygen. After the fluorine atom is substituted by the OH^-, the atomic configuration of the OH^- and surrounding atoms are re-optimized via a search of the total energy minimum as a function of the atomic displacements from the regular lattice sites.

3. Results and discussion

Firstly, we performed calculations of different configurations for the OH^- impurities in BaF_2 crystals. Considering the symmetry of alkaline-earth fluorides, we calculated three simple configurations in which the OH^- orients along the (100) or (111) direction. The (100)-oriented OH^- is labeled $OH_{(100)}$ in this paper. For the (111)-oriented case, there are two configurations named $OH_{(111)}$ (see Fig. 1) and $HO_{(111)}$. It is clear that the different orders of the oxygen and hydrogen atoms along the (111) direction correspond to the different OH^- configurations in BaF_2 crystals, as we can see Fig. 1. According to our calculations, we found that the energetically most favorable configuration of the OH^- impurity is Config $OH_{(111)}$, and the total energies of Configs $HO_{(111)}$ and $OH_{(100)}$ are larger than that of Config $OH_{(111)}$ by around 0.38 eV and 0.20 eV, respectively. We also simulated some other configurations with orientations slightly diverging the (111) axis and the results show that these configurations converge to Config $OH_{(111)}$ after geometrical relaxations via a search of the minimum total energy. Therefore, we mainly focus our current discussion on Config $OH_{(111)}$.

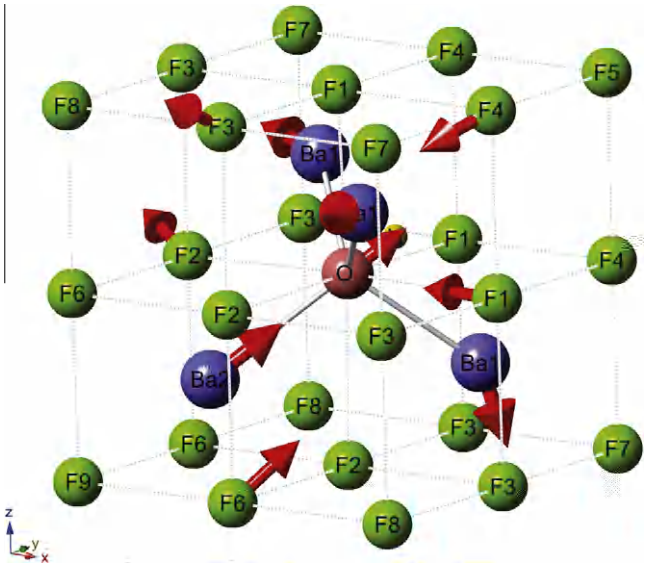

Fig. 1. A view of the OH^- oriented along the (111) axis for the $OH_{(111)}$ configuration. The arrows show the directions of the atomic displacements surrounding the OH^- impurity. According to the symmetries of the atoms, different labels are defined in spheres.

Next, we computed the geometrical property of OH^- and relaxation of atoms surrounding the OH^- impurity. The distances between the oxygen and hydrogen (or named the length of the OH^-) are 0.97 Å, 0.96 Å and 0.96 Å for Configs $OH_{(111)}$, $HO_{(111)}$ and $OH_{(100)}$, respectively. According to our calculations on H_2O molecule, Ca $(OH)_2$ and Ba $(OH)_2$ crystals, the lengths of OH^- are all around 0.96–0.97 Å, indicating that the OH^- has a steady geometrical structure in different materials. The calculation of the OH^- position in the BaF_2 bulk shows that one fluorine is substituted by an oxygen and a hydrogen occupies a neighbor interstitial site. For the (111)-oriented OH^-, the oxygen atom moves from the regular anion site backwards the neighbor barium along the (111) direction by 1.72% and 6.57% of a_0 for Configs $OH_{(111)}$ (see Fig. 1) and $HO_{(111)}$ respectively. The oxygen in Config $OH_{(100)}$ moves slightly along the (100) direction by less than 1% of a_0. The calculated atomic displacements of the OH^- and surrounding atoms for Config $OH_{(111)}$ are listed in Table 1. The three Ba1 atoms are repulsed from the OH^- by around 0.97% of a_0 and the Ba2 moves towards the OH^- by 0.84% of a_0. The relaxations of neighbor fluorine atoms are slight and less than 0.5% of a_0.

Table 1
Atomic relaxations (D ($\%a_0$): as a percentage of the lattice constant: 6.26 Å) and effective charges (Q (e)) of the OH^- and surrounding atoms in the BaF_2 96-atom supercell for Config $OH_{(111)}$. ΔQ (e) is the charge difference between the defective and perfect crystals ($Q_{Ba} = +1.845e$, $Q_F = -0.923e$ in perfect BaF_2). The shell labels have been defined in Fig. 1.

Atoms (*shell*)	Number	D ($\%a_0$)	Q (e)	ΔQ (e)
O	1	1.72	−1.033	–
H	1	–	+0.241	–
Ba1	3	0.97	+1.819	−0.026
Ba2	1	0.84	+1.840	−0.005
F1	3	0.20	−0.931	−0.008
F2	3	0.19	−0.928	−0.005
F3	6	0.32	−0.923	0
F4	3	0.22	−0.924	−0.001
F6	3	0.21	−0.923	0

Table 1 also presents the effective charges of the OH^- and surrounding atoms for Config $OH_{(111)}$. The total charge of the OH^-, i.e. the sum of the O and H charges, is $-0.792e$, being much smaller than the charge of the substituted fluorine atom ($-0.923e$) by $0.131e$. Around $0.083e$ and $0.039e$, localized on the four nearest Ba and six second-nearest F, respectively, transfer inward to the OH^-. For Configs $HO_{(111)}$ and $OH_{(100)}$, the effective charges of OH^- are $-0.785e$ and $-0.799e$, being close to the corresponding value of Config $OH_{(111)}$. We also calculated the OH^- charges in Ca $(OH)_2$ and Ba $(OH)_2$ crystals. The results show that the total effective charges of OH^- in Ca $(OH)_2$ and Ba $(OH)_2$ equal to $-0.781e$ and $-0.825e$ respectively. The OH^- charge in Ba $(OH)_2$ is larger than OH^- as impurities in BaF_2 crystal by around 0.3–0.4e and this phenomenon can be explained by the fact that the fluorine has a stronger oxidative property than that of OH^-. It is well known that the hydroxyl has a considerable covalency between the oxygen and hydrogen, which is also demonstrated by our bond population calculations for the OH^--BaF_2 systems. The presence of the covalency of OH^- in BaF_2 is also clearly shown in the charge density map (see Fig. 2). The covalent bonds between oxygen and hydrogen are 472me, 494m and 534me for Configs $OH_{(111)}$, $HO_{(111)}$ and $OH_{(100)}$, respectively. Compared with the covalent bonds in Ca $(OH)_2$ (458me) and Ba $(OH)_2$ (434me) crystals, the covalency of the OH^- impurities in BaF_2 is stronger than that in the hydroxide crystals. Here, we can conclude that OH^- as an atomic group has a steady geometrical structure rather than the electronic properties in different materials.

Alkaline-earth fluorides with defects degrade their optical quality and exhibit optical absorptions. Our calculations on the defect levels induced between the valence bands (VB) and conduction bands (CB) suggest a possible mechanism for the optical absorption. In the one-electron approximation scheme, the experimentally observed optical absorption could be due to an electron transition from the OH^--impurity ground state to the empty band induced by the OH^-. Our calculated band structure regarding the OH^--impurity system of Config $OH_{(111)}$ is shown in Fig. 3 and the optical band gaps for Configs $OH_{(111)}$, $HO_{(111)}$ and $OH_{(100)}$ are collected in Table 2. The optical band gaps between VB and CB for the BaF_2 96-atom supercells containing a OH^- at Γ point are 11.34 eV, 11.29 eV and 11.53 eV for Configs $OH_{(111)}$, $HO_{(111)}$ and $OH_{(100)}$ respectively, being close to the relevant gap of the perfect BaF_2 crystal (11.30 eV). For Config $OH_{(111)}$, the empty defect level induced by OH^- impurities is located 0.78 eV below the bottom of CB at Γ point (see Fig. 3). The occupied defect level, containing two superposed bands, induced by OH^- impurities are located 1.95 eV above the VB top at Γ point. Since hydroxyl has weaker oxidative property than that of fluorine, the hydroxy binding force to the outer-shell electrons is smaller, leading to the occupied OH^--bands shift upwards with respect to the VB top, mainly consisting of F outer p orbitals. From Fig. 3 and Table 2, we imply that the first optical absorption, corresponding to an electron transition from the occupied OH^--bands to the empty OH^--band, should be centered around 8.61 eV, being much larger than the relevant value of

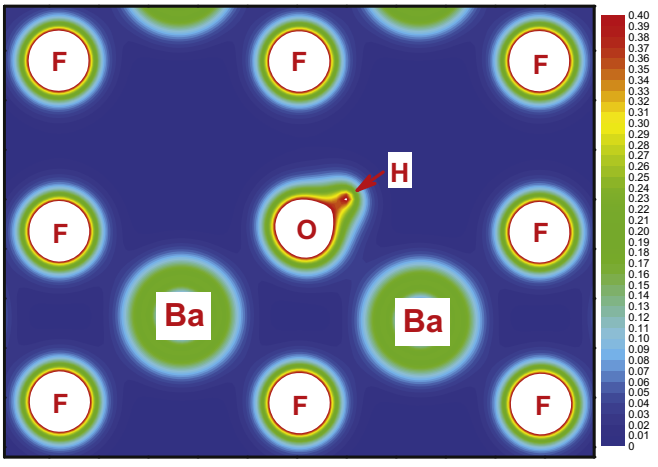

Fig. 2. Electron density contours in BaF_2 with OH^- from the (1 1 0) side view, being from 0 to 0.4e bohr^{-3} with a linear increment of 0.01e bohr^{-3}.

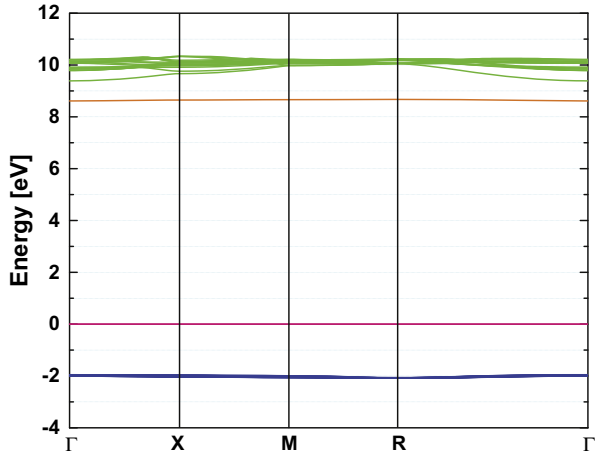

Fig. 3. Calculated B3PW band structure for the 96-atom supercell modeling the OH^- impurity in BaF_2 for Config $OH_{(111)}$.

Table 2
Direct optical band gaps (eV) ($\Gamma \rightarrow \Gamma$) for the OH^--impurity systems in Configs $OH_{(111)}$, $HO_{(111)}$ and $OH_{(100)}$.

Gaps	$OH_{(111)}$	$HO_{(111)}$	$OH_{(100)}$
O → H	8.61	8.59	8.98
O → CB	9.39	9.27	9.41
VB → H	10.56	10.61	11.10
VB → CB	11.34	11.29	11.53

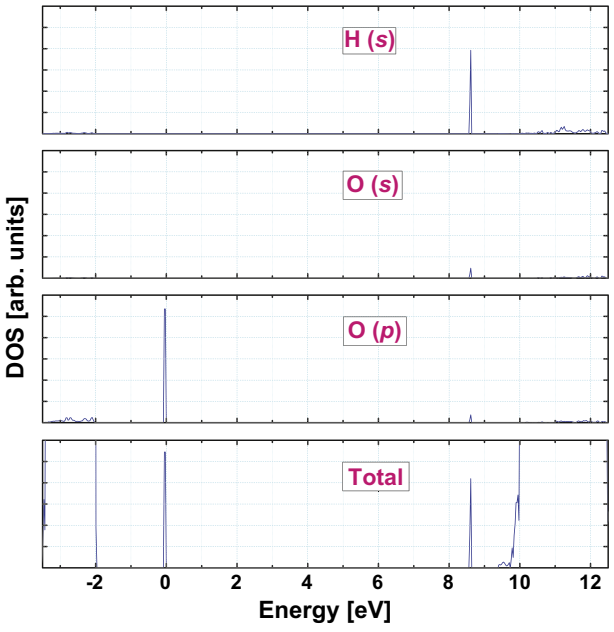

Fig. 4. Total and partial density of states (DOS) for the OH^- impurities (Config $OH_{(111)}$) in the BaF_2crystal.

4.27 eV for BaF_2 containing *F* centers (an electron trapped in the fluorine vacancy) [21]. It is because the trapped electron in the *F* center is more delocalized than the valence electron of hydroxyl.

To further study the electronic structure and electron transitions in a OH^--impurity system, we calculated the density of states (DOS) of the $OH_{(111)}$ system, as we can see Fig. 4. According to our calculation, the O *p* orbitals form the two superposed occupied OH^--bands, named O bands, and the H *s* orbitals do the major contribution to the empty defect band (so-called H band) below the CB bottom. Unlike the occupied O bands mainly consisting of only electrons localized on one kind of atoms, for the unoccupied H band, there are also innegligible contributions from O *s* and *p* orbitals.

4. Conclusions

We applied the first-principles approach within the hybrid DFT-B3PW scheme to calculations on OH^- impurities in BaF_2. Three OH^- configurations were studied and we found that Config $OH_{(111)}$, in which the hydroxyl orients the (111) axis and the oxygen occupies a regular fluorine site, is the energetically most favorable configuration for OH^--impurity systems. The length of OH^- impurity in BaF_2 crystal equals to around 0.97 Å, being close to the lengths of hydroxyl in water, Ca $(OH)_2$ and Ba $(OH)_2$, indicating a steady geometrical structure of hydroxyl. Effective charge analysis shows that some charges localized on the neighbor atoms (especially for the nearest barium atoms) transfer inward to the OH^-. The covalent bond between oxygen and hydrogen of the OH^- impurity in BaF_2 is stronger than that in Ba $(OH)_2$.

The studies on band structures and DOS of the OH^--impurity systems indicate that there are two defect levels induced by OH^- impurities in the VB-CB gap. The two superposed occupied O bands located 1.95 eV above the VB at Γ point mainly consist of the O *p* orbitals and the H *s* orbitals do the major contribution to the empty defect band located 0.78 eV below the CB bottom. According to our calculation, the first optical absorption, corresponding to an electron transition from the occupied O bands to the empty H band, is centered around 8.61 eV.

References

[1] K. Kawano, T. Ohya, T. Tsurumi, K. Katoh, R. Nakata, Phys. Rev. B 60 (1999) 11984.
[2] N. Sata, K. Eberman, K. Eberl, J. Maier, Nature 408 (2000) 946.
[3] J. Barth, R.L. Johnson, M. Cardona, D. Fuchs, A.M. Bradshaw, Phys. Rev. B 41 (1990) 3291.
[4] R. Bennewitz, D. Smith, M. Reichling, Phys. Rev. B 59 (1999) 8237.
[5] M. Catti, R. Dovesi, A. Pavese, V.R. Saunders, J. Phys.: Condens. Matter 3 (1991) 4151.
[6] W.Y. Ching, F.Q. Gan, M.Z. Huang, Phys. Rev. B 52 (1995) 1596.
[7] N.H. de Leeuw, T.G. Cooper, J. Mater. Chem. 13 (2003) 93.
[8] N.H. de Leeuw, J.A. Purton, S.C. Parker, G.W. Watson, G. Kresse, Surf. Sci. 452 (2000) 9.
[9] A.S. Foster, C. Barth, A.L. Shluger, R.M. Nieminen, M. Reichling, Phys. Rev. B 66 (2002) 235417.
[10] F.Q. Gan, Y.N. Xu, M.Z. Huang, W.Y. Ching, J.G. Harrison, Phys. Rev. B 45 (1992) 8248.
[11] A. Jockisch, U. Schroder, F.W. Dewette, W. Kress, J. Phys.: Condens. Matter 5 (1993) 5401.
[12] Y.C. Ma, M. Rohlfing, Phys. Rev. B 77 (2008) 115118.
[13] M. Merawa, M. Llunell, R. Orlando, M. Gelize-Duvignau, R. Dovesi, Chem. Phys. Lett. 368 (2003) 7.
[14] V.E. Puchin, A.V. Puchina, M. Huisinga, M. Reichling, J. Phys.: Condens. Matter 13 (2001) 2081.
[15] A.V. Puchina, V.E. Puchin, E.A. Kotomin, M. Reichling, Solid State Commun. 106 (1998) 285.
[16] G.W. Rubloff, Phys. Rev. B 5 (1972) 662.
[17] K. Schmalzl, D. Strauch, H. Schober, Phys. Rev. B 68 (2003) 144301.
[18] M. Verstraete, X. Gonze, Phys. Rev. B 68 (2003) 195123.
[19] X. Wu, S. Qin, Z.Y. Wu, Phys. Rev. B 73 (2006) 134103.
[20] H. Shi, R.I. Eglitis, G. Borstel, Phys. Rev. B 72 (2005) 045109.
[21] H. Shi, R.I. Eglitis, G. Borstel, J. Phys.: Condens. Matter 18 (2006) 8367.
[22] H. Shi, R.I. Eglitis, G. Borstel, J. Phys.: Condens. Matter 19 (2007) 056007.
[23] H. Shi, R.I. Eglitis, G. Borstel, Comput. Mater. Sci. 39 (2007) 430.
[24] R. Jia, H. Shi, G. Borstel, Phys. Rev. B 78 (2008) 224101.
[25] H. Shi, W. Luo, B. Johansson, R. Ahujia, J. Phys.: Condens. Matter 21 (2009) 415501.
[26] R. Bennewitz, D. Smith, M. Reichling, Phys. Rev. B 59 (1999) 8237.
[27] H. Shi, R. Jia, R.I. Eglitis, Phys. Rev. B 81 (2010) 195101.
[28] H. Adler, I. Kveta, S.B. Osterreich Akad. Wiss. Math.-Nat. Klasse. Abt II 199 (1957) 166.
[29] W. Bontinck, Physica 24 (1958) 650.
[30] A.D. Becke, J. Chem. Phys. 98 (1993) 5648.
[31] J.P. Perdew, Y. Wang, Phys. Rev. B 33 (1986) 8800.
[32] J.P. Perdew, Y. Wang, Phys. Rev. B 40 (1989) 3399.
[33] J.P. Perdew, Y. Wang, Phys. Rev. B 45 (1992) 13244.
[34] V.R. Saunders, R. Dovesi, C. Roetti, M. Causa, N.M. Harrison, R. Orlando, C.M. Zicovich-Wilson, CRYSTAL-2006 User Manual, University of Torino, Italy, 2006.
[35] S. Piskunov, E. Heifets, R.I. Eglitis, G. Borstel, Comput. Mater. Sci. 29 (2004) 165.
[36] R.I. Eglitis, S. Piskunov, E. Heifets, E.A. Kotomin, G. Borstel, Ceram. Int. 30 (2004) 1989.
[37] P.J. Hay, W.R. Wadt, J. Chem. Phys. 82 (1984) 299.
[38] R. Dovesi, C. Ermondi, E. Ferrero, C. Pisani, C. Roetti, Phys. Rev. B 29 (1984) 3591.
[39] H.J. Monkhorst, J.D. Pack, Phys. Rev. B 13 (1976) 5188.
[40] C. Pisani, Quantum-Mechanical Ab initio Calculations of the Properties of Crystalline Materials, Lecture Notes in Chemistry, vol. 67, 1996.